Virology 422 (2012) 425–434

Contents lists available at SciVerse ScienceDirect

Virology

journal homepage: www.elsevier.com/locate/yviro

First steps of bacteriophage SPP1 entry into *Bacillus subtilis*

Lina Jakutytė [a,b], Rudi Lurz [c], Catarina Baptista [d,e], Rut Carballido-Lopez [f], Carlos São-José [d,e], Paulo Tavares [a], Rimantas Daugelavičius [g,*]

[a] Unité de Virologie Moléculaire et Structurale, CNRS UPR3296 and IFR 115, Bâtiment 14B, CNRS, 91198 Gif-sur-Yvette, France
[b] Department of Biochemistry and Biophysics, Vilnius University, Čiurlionio 21, LT-03101 Vilnius, Lithuania
[c] Max-Planck Institut für Molekulare Genetik, Ihnestraße 63–73, D-14195, Germany
[d] Instituto de Medicina Molecular, Av. Prof. Egas Moniz, Ed. Egas Moniz, 1649–028 Lisboa, Portugal
[e] Unidade dos Retrovirus e Infecções Associadas, Centro de Patogénese Molecular, Faculdade de Farmácia da Universidade de Lisboa, Avenida das Forças Armadas, 1600–083 Lisboa, Portugal
[f] Institut National de la Recherche Agronomique, Unité Mixte de Recherche 1319 Micalis, Domaine de Vilvert, F-78352 Jouy-en-Josas, France
[g] Department of Biochemistry and Biotechnologies, Vytautas Magnus University, Vileikos 8, LT-44404 Kaunas, Lithuania

ARTICLE INFO

Article history:
Received 10 October 2011
Returned to author for revision
20 October 2011
Accepted 11 November 2011
Available online 6 December 2011

Keywords:
Bacteriophage SPP1
Virus entry
Ca^{2+} ions
Membrane voltage
Gram-positive bacterium
YueB

ABSTRACT

The mechanism of genome transfer from the virion to the host cytoplasm is critical to understand and control the beginning of viral infection. The initial steps of bacteriophage SPP1 infection of the Gram-positive bacterium *Bacillus subtilis* were monitored by following changes in permeability of the cytoplasmic membrane (CM). SPP1 leads to a distinctively faster CM depolarization than the one caused by podovirus ϕ29 or myovirus SP01 during *B. subtilis* infection. Depolarization requires interaction of SPP1 infective virion to its receptor protein YueB. The amplitude of depolarization depends on phage input and concentration of YueB at the cell surface. Sub-millimolar concentrations of Ca^{2+} are necessary and sufficient for SPP1 reversible binding to the host envelope and thus to trigger depolarization while DNA delivery to the cytoplasm depends on millimolar concentrations of this divalent cation. A model describing the early events of bacteriophage SPP1 infection is presented.

Introduction

Bacteriophages are obligate intracellular parasites like all viruses. Delivery of their genome to the host cell cytoplasm is thus an essential requirement for viral multiplication. In contrast to most eukaryotic viruses, the double-stranded DNA (dsDNA) of tailed phages enters the cytoplasm naked while the empty particle remains outside the bacterial envelope (Hershey and Chase, 1952). The barriers encountered by viruses of Eubacteria to reach the cytoplasm are the bacterial cell wall rigidified by a network of peptidoglycan (PG) and one or two membranes. Gram-negative bacteria are surrounded by an outer membrane containing lipopolysaccharides (LPS) followed by a thin (2.5 to 7.5 nm) PG layer and the cytoplasmic membrane (CM) (Silhavy et al., 2010). Gram-positive bacteria lack the outer membrane. They are surrounded by several layers of cross-linked PG that can reach a thickness of 50 nm. The second major component of Gram-positive cell walls are teichoic acids (WTA). The CM found underneath the cell wall is a highly selective hydrophobic barrier that controls the transport of different compounds between the cytoplasm of bacteria and the extracellular medium. The difference of electrical potential between the two aqueous solutions separated by the CM (membrane voltage, $\Delta\Psi$) is essential for the energized state of the cell (Nicholls and Ferguson, 2002). At an extracellular pH above 7 $\Delta\Psi$ is the main component of the proton-motive force. Depolarization of the CM due to inhibition of the respiratory chain or to the permeabilization of the membrane has a strong impact on the cell homeostasis and can lead to its death.

Bacteriophages use a variety of strategies to deliver their genome across the bacterial envelope to the cell cytoplasm where their genetic information is expressed and replicated (for a review see Poranen et al., 2002; Vinga et al., 2006a). Phage infection is initiated by the specific interaction of the virion with receptors at the host cell surface. The first contact with the bacterial surface usually leads to reversible binding. In a second step virions attach irreversibly to specific cell envelope receptors committing to infection of the host. Reversible and irreversible binding can be to the same receptor or involve different surface components, usually LPS, WTA and/or proteins (Vinga et al., 2006a and references therein). Phage particles frequently possess a cell wall degradation activity to drill the PG and to access the CM (Moak and Molineux, 2004). Phage genome passage through the CM requires formation of a pore preceding transfer of DNA from the virion to the cytoplasm. DNA entry can be a very fast process,

* Corresponding author. Fax: +370 37 327916.
E-mail address: r.daugelavicius@gmf.vdu.lt (R. Daugelavičius).

0042-6822/$ – see front matter © 2011 Elsevier Inc. All rights reserved.
doi:10.1016/j.virol.2011.11.010

e.g., it can take less than 30 seconds as found for phage T4 (Letellier et al., 1999), but can also be significantly slower as in the case of phage T7 whose complete genome internalization takes about one third of the infection cycle (Garcia and Molineux, 1996). Different durations of phage DNA entry likely result from diverse mechanisms of DNA transfer to the cytoplasm. Slow viral DNA entry limits genome accessibility in the cytoplasm providing a mechanism to maintain its integrity and to control sequential gene expression as reported for phages T7 and T5 (Garcia and Molineux, 1996; Lanni, 1968; Letellier et al., 1999; Zavriev and Shemyakin, 1982). Passage of viral DNA through the bacterial envelope is associated in most cases with a decrease of $\Delta\Psi$ and leakage of intracellular K^+ ions (Letellier et al., 1999; Poranen et al., 2002). Ion fluxes across the CM can be the result of creation of a hydrophilic channel for DNA passage or opening of existing channels in the CM triggered by phage infection.

Bacteriophage SPP1 is a siphovirus that infects the soil bacterium *Bacillus subtilis*. SPP1 binds preferentially at the bacterial pole which correlates with a preferential polar route for phage DNA entry (Jakutyte et al., 2011). Infection of SPP1 is initiated by reversible binding to poly(glycerophosphate) WTAs of the Gram-positive host (Baptista et al., 2008). The reversible phage binding facilitates scanning of the cell surface for irreversible attachment to the receptor YueB (Baptista et al., 2008). Most probably this membrane protein is a dimer. Each of its subunits has five carboxyl-terminal transmembrane segments and a large ectodomain forming a fiber that spans the cell wall and exposes the receptor domain at the cell surface (São-José et al., 2004, 2006). YueB is encoded by a putative type VII secretion system (T7SS) gene cluster of *B. subtilis* (Abdallah et al., 2007; São-José et al., 2004). The interaction of the SPP1 adsorption apparatus with YueB triggers a sequence of conformational changes in the phage tail structure (Plisson et al., 2007) that culminates in genome transfer from the viral capsid through the tail tube (São-José et al., 2006, 2007) into the host cytoplasm. Here we show that SPP1 binding leads to a very fast depolarization of the *B. subtilis* CM that requires the interaction of phage particles with YueB. The CM depolarization can be uncoupled from viral DNA entry into the cell. The depolarizing effect of SPP1 thus is a result of interaction between the phage particle and components of the cell envelope rather than of ions fluxes accompanying DNA traffic.

Results

SPP1 Interaction with B. Subtilis Causes a Very Fast Depolarization of the CM

The CM of bacterial cells is not permeable to inorganic ions like H^+ and K^+, but it is well permeable to lipophilic cations such as tetraphenylphosphonium (TPP^+). After addition of bacteria to TPP^+ containing medium, these cations cross rapidly the envelope of Gram-positive cells and distribute between the medium and the cytosol according to the electrical potential. At equilibrium the ratio of TPP^+ concentrations in the cytosol and in the medium provides a measure of $\Delta\Psi$. Therefore distribution of TPP^+ is used to follow the changes in membrane voltage of bacteria and mitochondria (Rottenberg, 1989).

The changes of TPP^+ concentration in the medium during the initial stages of SPP1 infection were monitored using a selective electrode. The medium composition, pH, and temperature of incubation were optimized to follow changes in the CM permeability during SPP1 infection. The strongest TPP^+ accumulation in *B. subtilis* cells, reflecting the highest $\Delta\Psi$, was observed when exponentially growing cells were transferred to 100 mM Tris–HCl, pH 8.0, but the SPP1-induced depolarization was weak (not shown). The maximal amplitude of depolarization was observed when the infection was performed in Luria–Bertani (LB) medium at pH 8.0 (not shown). This medium was supplemented with 5 mM $CaCl_2$ because Ca^{2+} ions play an important role in SPP1 infection (Santos et al., 1984). This concentration was used because 10 mM $CaCl_2$, the concentration usually used for SPP1 infection, led to lower TPP^+ uptake and reduced depolarization amplitude in response to SPP1 infection when compared to experiments carried out in presence of 5 mM $CaCl_2$. Gramicidin D (GD), an ionophore for monovalent cations (Nicholls and Ferguson, 2002), was added at the end of the assay for complete depolarization of the CM. All subsequent experiments were carried out in these conditions unless stated otherwise. The level of initial TPP^+ uptake and the magnitude of phage-induced CM depolarization showed some variation among bacterial cultures and during experiments using the same culture when the measurements were not carried out synchronously. Therefore, in most cases, parallel measurements were carried out in 4 vessels using the same initial culture. A weak repolarization of the membrane after SPP1-triggered depolarization was also observed in some experiments when the initial accumulation of TPP^+ was high and the phage-induced depolarization was weak but the depolarization was negligible in most of the experiments carried out.

SPP1 infection leads to depolarization of the CM of *B. subtilis* (Vinga et al., 2006b). The effects on $\Delta\Psi$ of other phages infecting the same host are not known. Therefore we studied accumulation of TPP^+ by YB886 cells infected in parallel with siphovirus SPP1 (Riva et al., 1968), podovirus ϕ29 (Anderson et al., 1966), and myovirus SP01 (Okubo et al., 1964) (Fig. 1A). Phage SPP1-induced depolarization starts within a few seconds after phage addition and proceeds very rapidly, the maximal depolarization being achieved at ~1 min post-infection (p.i.) (Fig. 1B). In the cases of phages ϕ29 and SP01 significantly longer lag periods were observed between phage addition and the start of depolarization. At 37 °C the maximal level of depolarization with phage SP01 was reached at ~3.5 min p.i., while phage ϕ29 caused a slow continuous efflux of TPP^+ ions from the cytosol of infected cells. At a lower temperature (27 °C), the kinetics of SPP1 induced TPP^+ efflux was only slightly slower, while for ϕ29 and SP01 a very weak leakage of the indicator cation was observed starting the 5th min of infection (Fig. 1C).

CM Depolarization Caused by SPP1 Infection Requires the Phage Receptor YueB and Depends on its Abundance at the Bacterial Surface

The fast depolarization of *B. subtilis* cells caused by SPP1 infection could be a result of the initial interaction between the virion and bacterial surface receptors. Therefore the TPP^+ efflux was monitored upon SPP1 interaction with three different *B. subtilis* strains: wild type cells (strain YB886), cells that do not synthesize the receptor YueB but allow reversible attachment of SPP1 particles to WTAs (Baptista et al., 2008; São-José et al., 2004), and cells that overproduce YueB (São-José et al., 2004) (Fig. 2A). No phage-induced leakage of TPP^+ was observed in cells lacking YueB indicating that the reversible phage binding to WTAs has no effect on the CM energetic state. In case of cells overproducing YueB the SPP1-induced depolarization had reproducibly higher amplitude than in wild type bacteria. This difference correlates with the significantly higher density of YueB at the surface of the overproducing cells (Jakutyte et al., 2011).

Since the amplitude of CM depolarization depends on the amount of YueB, we investigated the effect of the number of infective phage particles *per* bacterial cell (pfu/cfu) (input multiplicity; i.m.; Adams, 1959; Jakutyte et al., 2011) on depolarization of wild type and YueB-overproducing cells (Figs. 2B,C). The CM depolarization of wild type bacteria reached maximal amplitude at an i.m. of ~12 pfu/cfu being identical at higher i.m.s (Fig. 2B). The leakage of TPP^+ after GD addition indicated that the CM of infected cells remained considerably energized under these conditions. At i.m.s of 3 or above the depolarization observed for infections of the YueB overproducing cells was higher than the one observed for wild type bacteria when using the same i.m. (Fig. 2B, C). Furthermore, the increase in phage/bacterium ratio in YueB-overproducing cells correlated with an augmentation in the amplitude of depolarization until the

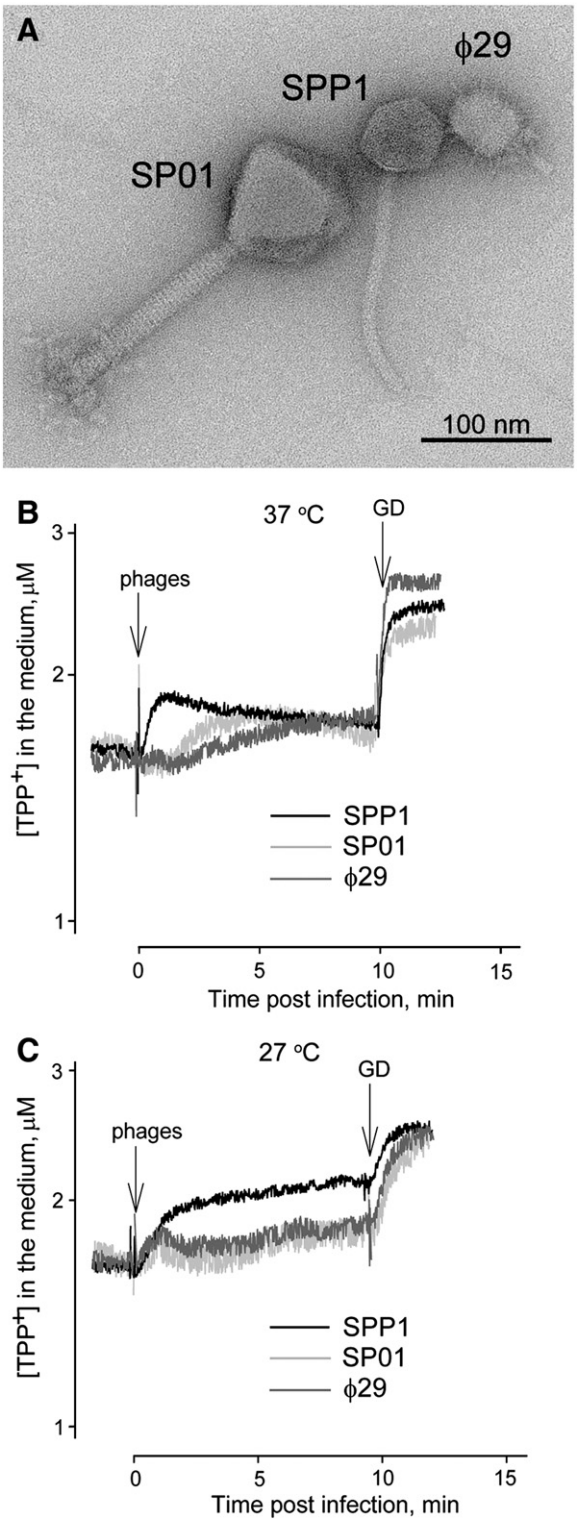

Fig. 1. Depolarization of the CM caused by SPP1, SP01 and ϕ29 infection of *B. subtilis* YB886. (A) SPP1, SP01 and ϕ29 phages observed by EM after negative staining. (B, C) Variation of extracellular TPP^+ concentration in cultures of *B. subtilis* YB886 cells infected with SPP1 (black), SP01 (light grey) and ϕ29 (dark grey) at 37 °C (B) and 27 °C (C). Infections were carried out at an i.m. of 6 pfu/cfu and the measurement of TPP^+ concentration in the medium was carried out as described in Materials and Methods. Arrows denote the addition of phages and GD (final concentration of 5 μg mL^{-1}). Similar results were obtained in three independent experiments.

complete CM depolarization was achieved at an i.m. of 48 (Fig. 2C). The SPP1 infection cycle progresses normally under these infection conditions with host cell lysis initiating at 30 min p.i. as found in infections at low i.m. (data not shown). Therefore, the strong CM depolarization does not result from immediate cell lysis due to simultaneous infection of each bacterium by a large number of SPP1 particles ("lysis from without"). The data show that the amplitude of CM depolarization depends on the number of SPP1 phage particles interacting with the cell (dependence on i.m.) and on the amount of YueB exposed on the cell surface for virions binding (dependence on YueB surface concentration) (Fig. 2B, C). The number of YueB receptors is a limiting factor for SPP1–induced CM depolarization in wild-type *B. subtilis*.

The finding that irreversible attachment of SPP1 to *B. subtilis* cells is strictly required to cause the CM depolarization led us to investigate if the binding of intact SPP1 particles to *B. subtilis* is sufficient to trigger this effect. SPP1 binding to the host is mediated by the tail adsorption apparatus localized at the tail end distal from the capsid (Plisson et al., 2007; São-José et al., 2006). The capacity of infectious phages and of intact tails to trigger depolarization was compared. In order to obtain tails, SPP1 particles were treated with EDTA that leads to dissociation of virions into free DNA, empty phages, empty capsids, and tails (Tavares et al., 1996). The resulting tails maintained intact their cell surface binding apparatus (arrows in Fig. 3A). They kept also their capacity to bind to *B. subtilis* with the same efficiency as wild type phages as assessed by counting intact and disrupted viral particles labeled with quantum dots that remain associated to bacteria after dilution and centrifugation of phage-cells complexes (Fig. 3B). However, disrupted phage structures did not cause any detectable leakage of TPP^+ when an equivalent of 5 to 50 disrupted particles per bacterium was tested (Fig. 3C; data not shown). This result indicates that attachment of the intact SPP1 particles is required to trigger the CM depolarization.

Effects of Ca^{2+} Ions on SPP1 Infection

Divalent cations play a key role in bacteriophage infection (Bonhivers and Letellier, 1995; Cvirkaite-Krupovic et al., 2010; Landry and Zsigray, 1980; Steensma and Blok, 1979). In case of SPP1 the highest efficiencies of plating (e.o.p.) are obtained in the presence of 10 mM Ca^{2+} (100%) and, in decreasing order, with Sr^{2+} (70 to 80%) and Mg^{2+} (40 to 60%) (Santos et al., 1984). This raised the question of which step(s) of SPP1 infection depend(s) on the presence of extracellular divalent cations. A detailed analysis of the SPP1 e.o.p. in semi-solid medium showed a reduction to ~60% when the concentration of added $CaCl_2$ was reduced from 10 to 5 mM (Fig. 4A). The e.o.p. is severely compromised at concentrations of 1 mM $CaCl_2$ and results also in a marked decrease of phage plaque size (Fig. 4B). No SPP1 plating was observed in the absence of exogenous Ca^{2+} added to the LB medium that contained 10 μM Ca^{2+}, as measured using a Ca^{2+} sensitive electrode (data not shown). This strong dependence on Ca^{2+} explains some variations observed among different laboratories when the e.o.p. of SPP1 is determined in absence of divalent cations (our unpublished results). Most probably they are due to different trace amounts of Ca^{2+} found in LB medium and water.

No SPP1 irreversible binding to *B. subtilis* cells in LB medium could be measured when Ca^{2+} ions were depleted by addition of 0.5 mM EGTA (Fig. 4C). We observed that the SPP1 irreversible adsorption constant (k_{ads}) was directly proportional to the logarithm of $CaCl_2$ concentration in the range between 0.25 and 10 mM (inset in Fig. 4C). Since the rate of irreversible binding is highly conditioned by the reversible interaction of SPP1 with WTA (Baptista et al., 2008) we also studied dependence of the latter type of binding on Ca^{2+} concentration. Again, Ca^{2+} depletion from LB by EGTA resulted in very low reversible binding, particularly when scored at 37 °C that favors dissociation of the reversibly bound phages (Fig. 4D; Baptista et al., 2008). However, the micromolar Ca^{2+} concentrations present in LB medium were sufficient to sustain reversible binding of more than 90% of the phage input at conditions that disfavor phage

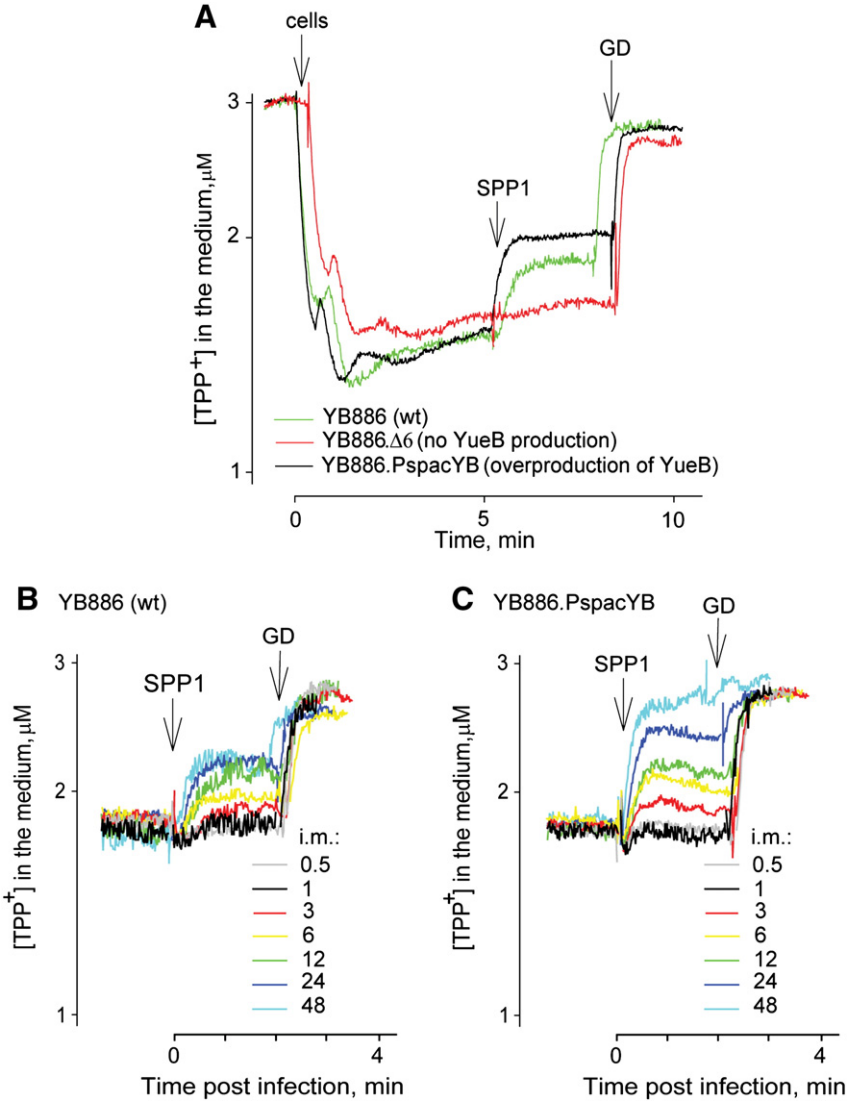

Fig. 2. Effect of SPP1 infection on TPP^+ ion fluxes across the CM of different *B. subtilis* strains. (**A**) Infection (i.m. of 5 pfu/cfu) of wild type YB886 (green), YB886.Δ6 (no YueB production) (red), and YB886.PspacYB (overproduction of YueB) (black). Similar results were obtained in three independent experiments. Effect of i.m. (pfu/cfu; as indicated in B and C) on SPP1-induced TPP^+ ion fluxes across the CM of *B. subtilis* YB886 (B) and YB886.PspacYB (C). Similar results were obtained in two independent experiments.

desorption (0 °C, Baptista et al., 2008). At both temperature equilibrium states we observed that the levels of reversibly associated phage particles were higher as the Ca^{2+} concentration increased (Fig. 4D). However, these results do not allow discriminating whether Ca^{2+} is necessary exclusively for reversible binding to glucosylated teichoic acids, a requirement for efficient irreversible binding of SPP1 to YueB in liquid medium, or if the divalent cations also play a role directly in phage/YueB interaction.

Depletion of Ca^{2+} that abolished SPP1 binding to *B. subtilis* prevented also phage-induced CM depolarization. This inhibition was readily overcome when EGTA was titrated by the 230 μM Ca^{2+} concentration measured to be present in the LB medium used for TPP^+ measurements (concentration of EGTA ≤ 0.05 mM) or by addition of exogenous Ca^{2+} (EGTA ≥ 0.05 mM) (Fig. S1). Surprisingly, the amplitude of SPP1-induced TPP^+ efflux was higher in LB medium containing 230 μM Ca^{2+} than in the presence of 5 mM Ca^{2+} (Fig. 5). Experiments performed at different i.m.s showed that the increase in phage/bacterium ratio led to the expected increase in amplitude of phage–induced depolarization (Fig. 5). In LB medium supplemented with 5 mM Ca^{2+} the maximal amplitude of CM depolarization was reached at an i.m. of ~8 but no complete depolarization was observed (Fig. 5A). In LB medium without additional Ca^{2+} the amplitude of depolarization was significantly higher leading to almost complete CM depolarization at i.m.s ≥ 8 (Fig. 5B). The CM depolarization caused by SPP1 thus requires the presence of micromolar concentrations of Ca^{2+}, while millimolar concentrations are inhibitory. The amplitude of SPP1-induced TPP^+ efflux in presence of 5 mM $CaCl_2$ was lower than in the presence of the same concentrations of $MgCl_2$, $BaCl_2$ or $SrCl_2$ (not shown) indicating that the effect of Ca^{2+} on SPP1-induced depolarization of the CM is specific.

A leakage of cytosolic K^+ usually takes place concomitantly with phage infection (Cvirkaite-Krupovic et al., 2010; Gaidelyte et al., 2006; Letellier et al., 1999). The addition of SPP1 particles to *B. subtilis* cell suspensions led to a very slow efflux of K^+ ions (Fig. 6A) when compared to SPP1-induced leakage of TPP^+ (Fig. 6B). The magnitude of K^+ leakage from SPP1-infected cells in LB containing 230 μM Ca^{2+} was higher than in LB supplemented with 5 mM Ca^{2+} as observed also for CM depolarization. These results suggest that SPP1 does not induce K^+ permeable channels upon infection and the slow leakage of K^+ is a result of the CM depolarization.

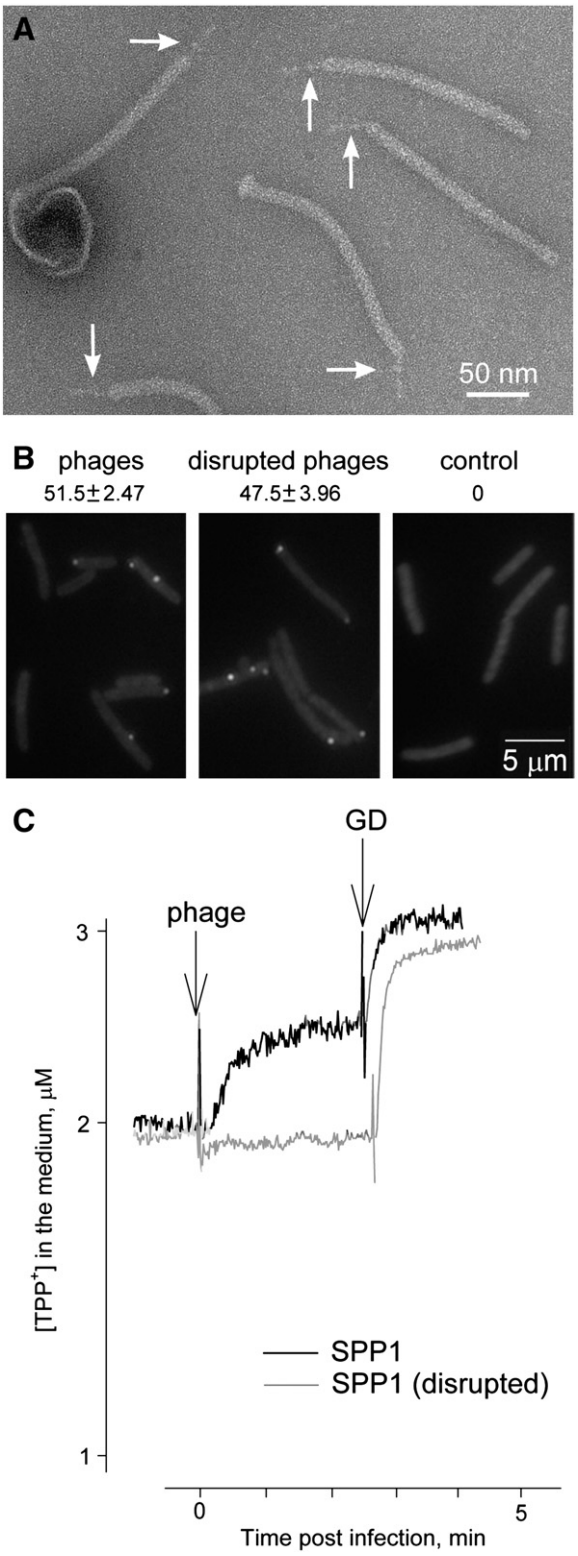

Fig. 3. TPP^+ ion fluxes across the CM of *B. subtilis* YB886 incubated with viable and disrupted SPP1 virions. (A) SPP1 phages disrupted with EDTA observed by EM after negative staining. Note that the host adsorption apparatus characterized by presence of the tail spike remains intact (arrows). (B) Phages (left) and disrupted phages (center) labeled with quantum dots binding to *B. subtilis* YB886. No unspecific binding of quantum dots to bacteria was observed (right). (C) Measurement of TPP^+ concentration in the medium of cells challenged with intact (i.m. of 5 pfu/cfu) or with an equivalent number of EDTA-disrupted particles. Similar results were obtained in three independent experiments.

According to the e.o.p., effective SPP1 infection requires Ca^{2+} concentrations above 1 mM while detectable reversible binding of phage particles to *B. subtilis* occurs at sub-millimolar Ca^{2+} concentrations (Fig. 4). This observation indicates that in addition to the effect of reversible binding Ca^{2+} is necessary at later steps of SPP1 infection cycle. We have investigated if Ca^{2+} ions are necessary for phage DNA transfer from the virion into the *B. subtilis* cytoplasm. GSY10000 cells producing a LacI-CFP soluble fusion were infected with phage SPP1*delX110lacO*$_{64}$ that carries an array of 64 *lacO* repeats in its genome (Jakutyte et al., 2011). The appearance of intracellular fluorescent foci whose size and intensity increases with time shows that viral DNA has entered and replicates in the cytoplasm. When *B. subtilis* GSY10000 cells were infected with SPP1*delX110lacO*$_{64}$ at an i.m. of 5 in presence of 5 mM $CaCl_2$, as used in TPP^+ measurements, 65 ± 9.7% of the cells had an intracellular fluorescent focus (Fig. 7A, E). Percentage of cells having foci decreased to 20.3 ± 6.6%, when concentration of $CaCl_2$ was decreased to 1 mM (Fig. 7B, E). In presence of sub-millimolar $CaCl_2$ concentrations appearance of fluorescent phage DNA foci was strongly affected: only 4.5 ± 3% and 1.1 ± 0.3% of infected cells had fluorescent DNA foci in presence of additional 0.25 mM or without additional $CaCl_2$, respectively (Fig. 7C, D, E).

Discussion

Virus genome entry into bacteria requires crossing of the cell envelope. This initial step of infection is usually associated with depolarization of the CM and/or the release of intracellular K^+ ions (Letellier et al., 1999; Poranen et al., 2002). The timing and pattern of ion leakage is different among phages, providing a fingerprint for infection by each virus species. It is not known, if depolarization of the CM and/or K^+ leakage play a physiological role in infection or if they are side effects accompanying phage entry. Infection of *Escherichia coli* by tailed phages T4 and T5 leads both to the CM depolarization and to the K^+ efflux (Boulanger and Letellier, 1992; Grinius and Daugelavicius, 1988; Labedan and Letellier, 1981; Letellier and Labedan, 1984). In contrast, bacteriophage PRD1 that uses an internal membrane device for DNA delivery to the host cytoplasm leads to an efflux of K^+ but no membrane depolarization is observed during phage entry (Daugelavicius et al., 1997; Grahn et al., 2002). Bacteriophage SPP1 binding to *B. subtilis* leads to a rapid (<1 min) depolarization of the host CM (Fig. 6B) but only to a slow and weak leakage of intracellular K^+ (Fig. 6A). SPP1-induced depolarization is significantly faster than the one accompanying infection of *B. subtilis* by tailed phages ϕ29 and SP01 or entry of the membrane-containing phage Bam35 into *B. thuringiensis* (Gaidelyte et al., 2006). In the latter case the CM depolarization and the leakage of intracellular K^+ occur simultaneously starting at 2 min p.i. SPP1-induced CM depolarization also shows a reduced temperature-dependence compared to the three other phages discussed (Fig. 1C; Gaidelyte et al., 2006). The reason of phage-induced event sensitivity to temperature could be dependence on the enzymatic processes and/or on the membrane fluidity. The delays of ϕ29 and SP01 (Fig. 1B) or Bam35 (Gaidelyte et al., 2006)-induced TPP^+ leakages at 27 °C indicate at least one temperature-dependent step of phage entry that is facilitated in case of SPP1 infection. A possible candidate is the cell wall digestion following the irreversible binding to non-proteinaceous receptors: ϕ29 and SP01 attach to WTA (Yasbin et al., 1976; Young, 1967) while Bam35 binds to *N*-Acetyl-muramic acid (Gaidelyte et al., 2006).

SPP1 attaches reversibly to glucosylated WTA (Baptista et al., 2008), but this step does not lead to the CM depolarization. The binding of SPP1 particles to YueB (Fig. 2), a CM protein whose ectodomain spans the complete cell wall to expose the SPP1 receptor region (São-José et al., 2004, 2006) is required to trigger depolarization. The level of *B. subtilis* CM depolarization increases with the i.m. (Fig. 2B) showing that each phage irreversible binding event generates a depolarizing signal. The maximal amplitude of depolarization for the wild type

B. subtilis strain YB886 was reached at an i.m. of 8 SPP1 virions per bacterium. The observed SPP1-induced CM depolarization was only partial, reflecting a limited number of active YueB receptors for phage binding at the bacterial surface (Baptista et al., 2008; Jakutyte et al., 2011; São-José et al., 2004). This conclusion is supported by infection of YueB-overproducing cells when higher amplitudes of TPP^+ efflux are registered which can reach values revealing total depolarization of the CM (Fig. 2C). The trigger for CM depolarization requires the interaction of intact SPP1 particles with *B. subtilis* (Fig. 3B). These results indicate that some structural modification in the SPP1 particle, probably the initiation of DNA ejection, is necessary signal for opening/formation of depolarizing channel(s). This differs from phage T4 whose intact virions and particles disrupted by osmotic shock (ghosts) both cause ion efflux upon interaction with host bacteria (Boulanger and Letellier, 1988; Duckworth and Winkler, 1972; Winkler and Duckworth, 1971).

Ca^{2+} ions play an essential role at early stages of infection by phages of the SPP1 group (Landry and Zsigray, 1980; Santos et al., 1984; Steensma and Blok, 1979; Figs. 4 and 7). Here we show that the divalent cations are necessary for phage reversible binding to glucosylated WTAs (Fig. 4D). WTAs together with teichuronic acids are the prime site metal binders in *B. subtilis* accounting for Ca^{2+}concentration at the cell wall 100–120-fold higher than in the extracellular medium (Neuhaus and Baddiley, 2003; Petit-Glatron et al., 1993). The effect of the divalent cations on WTA structure (Neuhaus and Baddiley, 2003) and/or on local cell wall surface charge might explain their role on SPP1 reversible binding to the *B. subtilis* envelope. Present data do not allow establishing if Ca^{2+} plays also a role in the subsequent irreversible interaction of SPP1 with YueB that commits the viral particle to infection. Binding of SPP1 to *B. subtilis* requires sub-millimolar concentrations of Ca^{2+} that are also sufficient for SPP1 particles to trigger the CM depolarization (Fig. 5). Raising extracellular Ca^{2+} concentration to millimolar levels is essential for effective SPP1 DNA entry into the cytoplasm (Fig. 7) and for achievement of productive infection as determined by the efficiency of plating in solid medium (Fig. 4A, B). The amplitude of CM depolarization decreases at this Ca^{2+} concentration, revealing an inhibitory effect on permeabilization of the CM (Figs. 5 and 6) that might contribute to maintenance of homeostasis in the infected *B. subtilis* cell. Ca^{2+} ions were also shown to act on the structure of tail adsorption apparatus from phage particles infecting Gram-positive bacteria. Their presence triggers a dramatic conformational switch in the isolated baseplate of lactococcal phage p2 that leads to opening of the structure, likely mimicking the structural rearrangement allowing phage genome release from virions (Sciara et al., 2010). The SPP1 related structure (gp19.1–$gp21_{1-552}$ complex; Goulet et al., 2011) is localized in the cap region of the tail tube end that opens for DNA exit of the virion to enter the host cell at the beginning of infection (Plisson et al., 2007; Veesler et al., 2010). Interestingly, Ca^{2+} stabilizes the open conformation of the gp19.1–$gp21_{1-552}$ complex found in the post-DNA ejection state of SPP1 virions (Goulet et al., 2011). The ensemble of the data indicates that Ca^{2+} ions might act both in the bacterial envelope and in the virion structure to support different steps necessary for phage DNA delivery to the host cytoplasm.

The results described here define a sequence of discrete steps necessary for SPP1 passage through the Gram-positive envelope of *B. subtilis* (Fig. 8). SPP1 adsorption to *B. subtilis* that culminates in irreversible binding to YueB requires sub-millimolar amounts of Ca^{2+} (steps 1–2 in Fig. 8). This interaction leads to a very fast depolarization of the CM strongly suggesting opening of a transmembrane

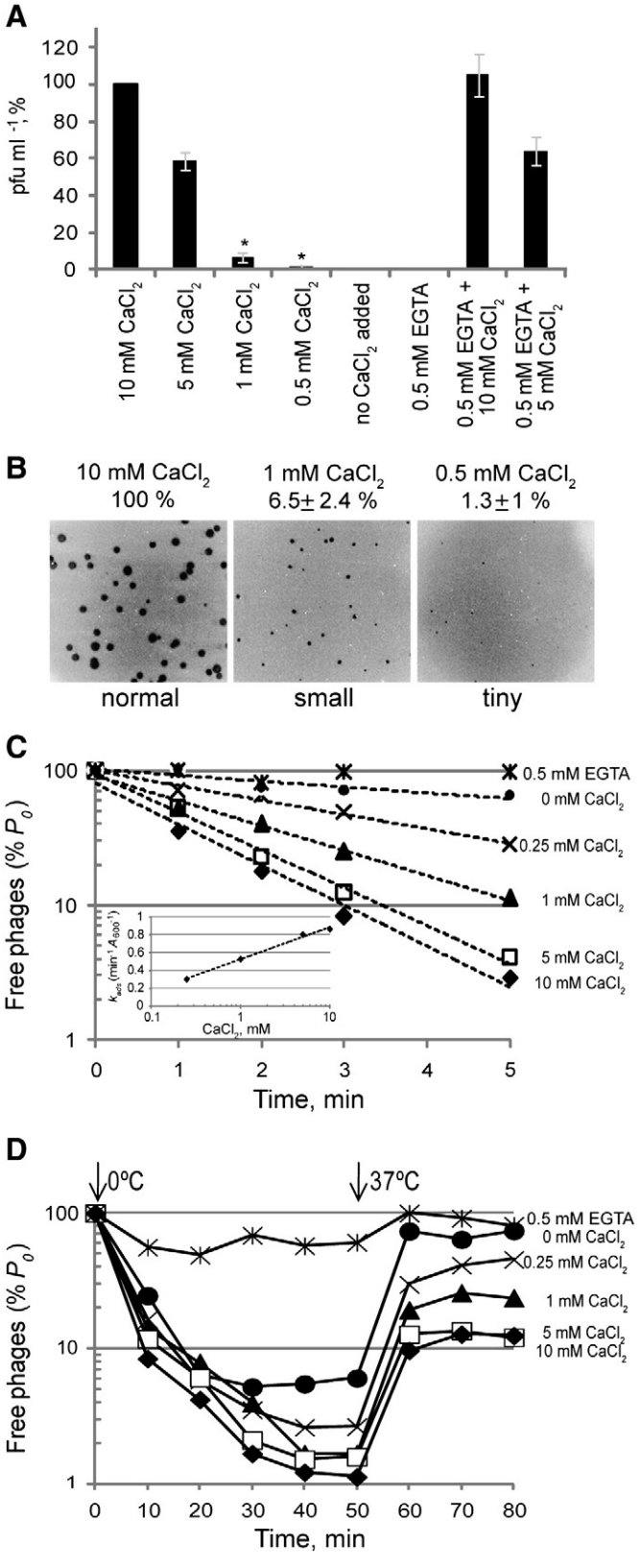

Fig. 4. Effect of Ca^{2+} on SPP1 infection. (A) SPP1 infection of *B. subtilis* YB886 in semi-solid medium (e.o.p.) containing the supplements indicated. The titers are expressed as percentage of the titer obtained in presence of 10 mM $CaCl_2$ ($1.62\times10^{12}\pm3.29$ pfu/mL) and are averages of at least 3 independent experiments. The asterisk indicates a small plaque phenotype dependent on the $CaCl_2$ concentration as illustrated in (B). (C) SPP1 irreversible adsorption to *B. subtilis* YB886. The irreversible adsorption constant (k_{ads}), determined as described (Baptista et al., 2008), was plotted against the log of $CaCl_2$ concentration (inset). (D) SPP1 reversible adsorption. *B. subtilis* YB886.Δ6 (no YueB production) in presence of the indicated $CaCl_2$ concentrations was pre-incubated in melting ice for 10 min. SPP1 was added (i.m. of 0.1) and aliquots taken at different time points to score for viable virions in the culture supernatant as described (Baptista et al., 2008). The culture was switched to 37 °C at 50 min post-infection to favor release of adsorbed phages. Results are plotted as percentage of the initial phage input (P_0).

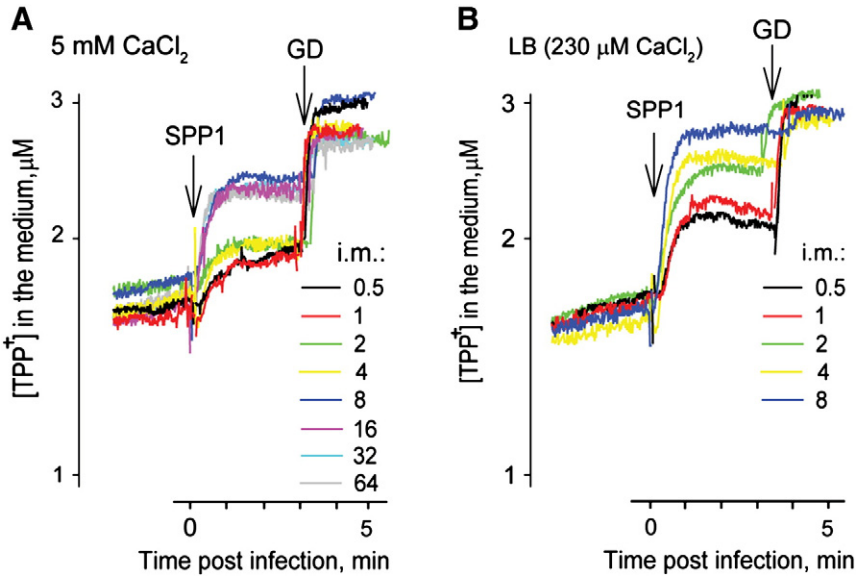

Fig. 5. Dependence of SPP1-induced CM depolarization on Ca^{2+} concentration. Infections were carried out in LB containing 5 mM $CaCl_2$ (A) or without supplement (containing 230 μM Ca^{2+} in the extracellular LB medium as measured with a Ca^{2+} electrode) (B) at the i.ms indicated. Similar results were obtained in three independent experiments.

channel whose identity remains to be established. The correlation between the amplitude of depolarization and the amount of phage-YueB complexes on the cell surface (Fig. 2) suggests that such channel could be (i) formed by the transmembrane segments of YueB (depicted by the conformational switch of YueB between steps 2 and 3 in Fig. 8), (ii) formed by a cellular protein associated to YueB (yellow in Fig. 8), or (iii) formed by YueB-independent phage or cell protein (pink channel in step 3 in Fig. 8). The first two ways of the CM depolarization imply signal transduction through the YueB structure while the third one contemplates an YueB-independent action of the viral particle targeting the CM. The requirement for intact viral particles to trigger depolarization (Fig. 3) indicates that channel opening/formation depends on a stimulus from the virion bound to YueB. Initiation of the cascade of structural rearrangements leading to DNA ejection from SPP1 particles (depicted by the open interior of the tail from step 3 on in Fig. 8) (Raspaud et al., 2007) is the most conceivable possibility. However, the trigger of depolarization is not obligatorily linked to successful transfer of SPP1 DNA to the host cytoplasm because the two events can be uncoupled at sub-millimolar concentrations of extracellular Ca^{2+} (Figs. 5 and 7). Opening of the hydrophilic channel(s) for membrane depolarization and DNA passage is directly or indirectly regulated by the divalent cations. A Ca^{2+}-dependent switch of channel structure is likely at least in the case of ion fluxes leading to depolarization and DNA traffic occuring through the same channel. Deletion of YueB carboxyl terminus transmembrane segments still allows for SPP1 infection in semi-solid medium, but not in liquid medium which hampered TPP^+ measurements (C.S.-J. and Mário A. Santos, unpublished results), suggesting that the receptor protein does not provide the route for phage DNA passage through the CM. Access of the phage particle to the CM usually requires a localized cell wall degradation, but this process not yet documented for SPP1 (step 4 in Fig. 8). The last step is phage DNA delivery to the cytoplasm through a hydrophilic channel formed in the CM either by phage or host protein(s) (step 5). The goal is now set to identify the phage and host effectors acting on these different steps that will provide a framework to understand in molecular detail how SPP1 crosses the Gram-positive cell envelope.

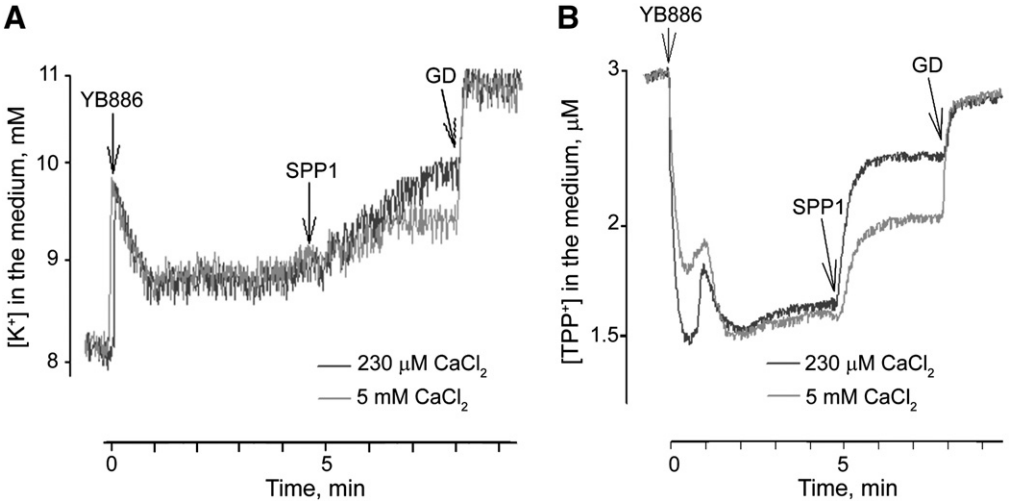

Fig. 6. K^+ (A) and TPP^+ (B) ion fluxes across the CM of *B. subtilis* infected with SPP1 (5 pfu/cfu) when no Ca^{2+} is added (black) and in presence of exogenous 5 mM $CaCl_2$ (grey). Extracellular ion concentrations were measured with ion specific electrodes. Similar results were obtained in three independent experiments.

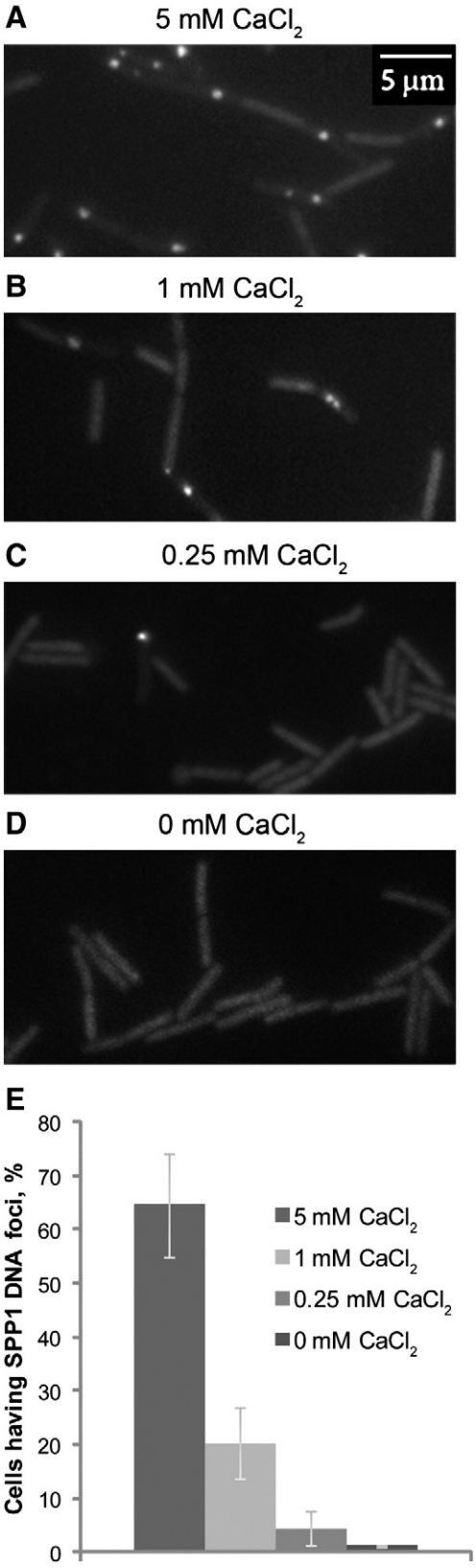

Fig. 7. Visualization of SPP1 DNA in *B. subtilis* infected cells. (A–D) Cultures of *B. subtilis* producing LacI-CFP supplemented with 5 (A), 1 (B), 0.25 mM $CaCl_2$ (C) and without additional $CaCl_2$ (D), infected by phage SPP1*delX110lacO*$_{64}$ (5 pfu/cfu), and imaged at 20–40 min p.i. (E) Percentage of cells having SPP1 DNA foci after 20–40 min of infection in presence of the supplements indicated. Results are from four independent infection experiments in which a total number of 412 (A), 525 (B), 634 (C) and 405 (D) cells were counted.

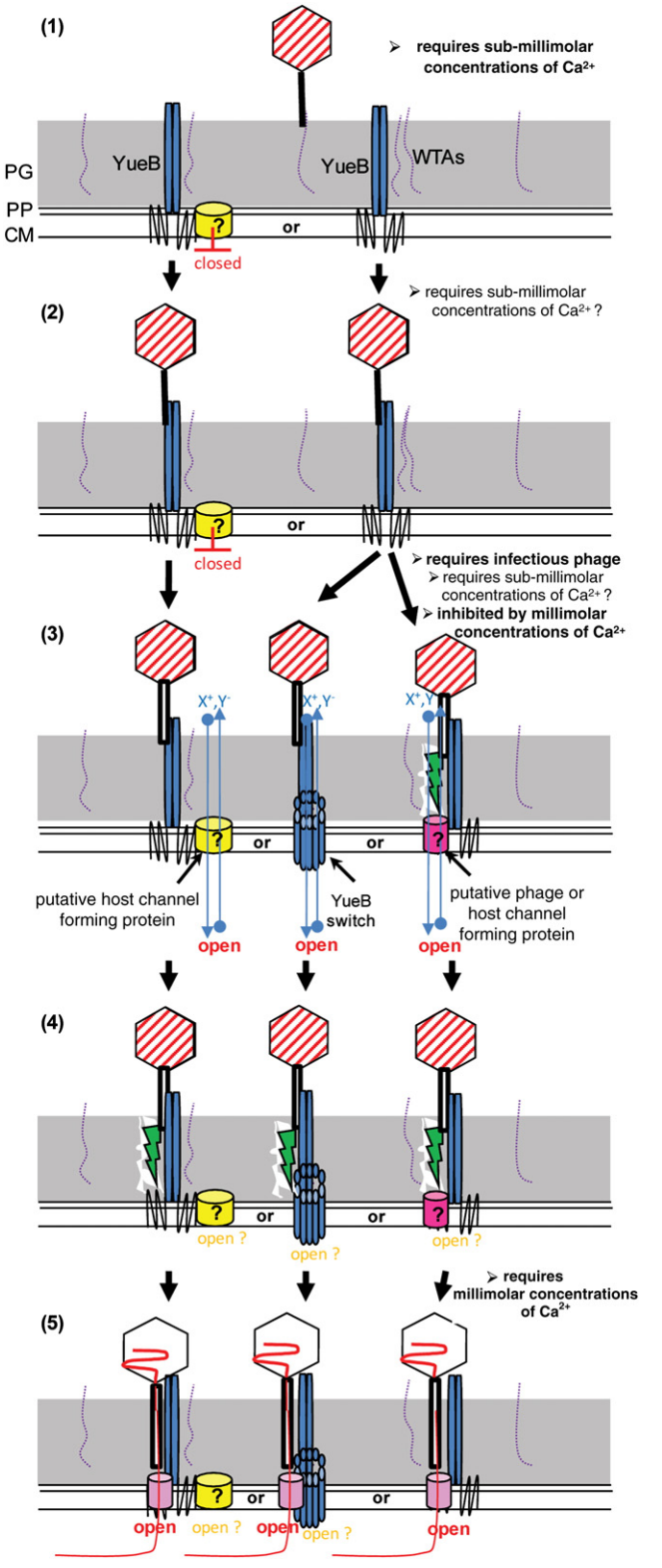

Fig. 8. Model for SPP1 entry into the host cell. (1) Reversible adsorption to glucosylated cell wall teichoic acids (WTAs). PG — peptidoglycan layer; PP — periplasm; CM — cytoplasmic membrane. (2) Irreversible adsorption to YueB. (3) Structural modification in the SPP1 phage; generation of signal to trigger CM depolarization. X^+ — positively charged ions; Y^- – negatively charged ions. (4) Cell wall localized degradation. (5) DNA passage through the CM and entry in the cytoplasm. Requirements for Ca^{2+} for each SPP1 entry step are indicated. Details on the ion channels depicted are described in the text.

Table 1
B.subtilis strains and phages used in this work.

Strains, phages	Genotype and/or relevant features[a]	Reference
B. subtilis strains		
YB886	*B. subtilis* 168 derivative freed of prophages PBSX and SPβ; wild-type strain; SPP1 indicator strain	(Yasbin et al., 1980)
YB886.Δ6	YB886 derivative with deleted *yueB* (Δ6 deletion). Contains an *eryR* marker inserted in the *amyE* locus; Ery^r (0.5 μg mL^{-1})	(Jakutyte et al., 2011)
YB886.PspacYB	YB886 derivative expressing *yueB* under the control of the promoter P_{spac} (inducible with IPTG); Ery^r (0.5 μg mL^{-1})	(Jakutyte et al., 2011)
GSY10000	YB886 derivative; expression of *lacI-cfp*; *thrC*::P_{pen}-*lacIΔ11-cfp(W7) mls* Ery^r (0.5 μg ml^{-1}) Lin^r (12.5 μg ml^{-1})	(Jakutyte et al., 2011)
12A	Asporogenic strain; *trpC2 spoOA12*	(Hoch and Spizizen, 1969)
B. subtilis phages		
SPP1	Lytic *B. subtilis* siphophage	(Riva et al., 1968)
SPP1*ΔX110lacO*$_{64}$	SPP1 derivative carrying deletion *delX* (Tavares et al., 1992) and an array of *lacO* operators	(Jakutyte et al., 2011)
SP01	Lytic *B. subtilis* myophage	(Okubo et al., 1964)
ϕ29	Lytic *B. subtilis* podophage	(Anderson et al., 1966)

[a] Ery^r, erythromycin resistance, Lin^r, lincomycin resistance.

Material and Methods

General Methods

B. subtilis strains and phages used in the present study are listed in Table 1. *B. subtilis* was grown in LB medium supplemented with appropriate antibiotic(s) (Table 1). Phages SPP1 and SP01 were multiplied in *B. subtilis* YB886 (Yasbin et al., 1980) and phage ϕ29 in *B. subtilis* 12A (Hoch and Spizizen, 1969) grown in LB medium supplemented with 10 mM $CaCl_2$ (for SPP1, SP01 and ϕ29) and 10 mM $MgCl_2$ (for ϕ29) (Chen and Guo, 1997; Santos et al., 1984) prior to infection. Phage multiplication and purification were carried out as described (Jakutyte et al., 2011).

Measurements of Ion Fluxes

The protocols of Daugelavicius et al. (1997) and Vinga et al. (2006b) were used to measure ion fluxes during phage infection of *B. subtilis* with the following modifications. To investigate the early changes in the CM permeability of phage infected cells, overnight cultures of *B. subtilis* were diluted 1:50 in fresh LB medium, pH 8.0 (pH adjusted with NaOH), supplemented with appropriate antibiotics (Jakutyte et al., 2011) and grown at 37 °C to exponential phase (A_{600} of 0.8). The cells were collected by centrifugation, and resuspended in LB, pH 8.0, to obtain a ~150-fold concentration of the original cell culture volume. Bacteria were kept at room temperature and used within 4 h. 2.5×10^9 cfu were added to two-four 5 mL thermostated (37 °C) and magnetically stirred reaction vessels containing 5 mL of LB, pH 8.0, supplemented with 3 μM TPP^+ and 5 mM $CaCl_2$, incubated for 5 min, and infected. Phages were added at the desired i.m.. At the end of the experiment the CM was permeabilized by addition of GD to a final concentration of 5 μg mL^{-1}. Full depolarization of the membrane allowed to estimate the amount of TPP^+ accumulated inside the cells in an ΔΨ-dependent way and the amount of this cation irreversibly bound to the cell envelope (difference between the initial 3 μM and the final TPP^+ concentration after GD-caused TPP^+ released to medium) (Daugelavicius et al., 1997). The concentrations of TPP^+, K^+ and Ca^{2+} in the medium were monitored using selective electrodes as described previously (Gaidelyte et al., 2006; Vinga et al., 2006b). TPP^+ chloride and GD were purchased from Sigma.

SPP1 Phages Disruption

CsCl-purified phage particles were disrupted by incubation with 50 mM EDTA, pH 8.0, at 55 °C for 30 min (Tavares et al., 1996). After addition of 100 mM $MgCl_2$, DNA was digested for 1 h at 37 °C with 0.4 U μL^{-1} of Benzonase (Merck). SPP1 particles were treated in parallel under the same conditions except that no EDTA was added to be used as control in all experiments carried out with the disrupted particles. Phage particles (100 μL) were diluted into 5 mL of LB medium containing 5 mM $CaCl_2$ for TPP^+ measurements leading to a residual input of 1 mM EDTA and 2 mM Mg^{2+} ions in the medium mix.

Electron Microscopy

Phages and phage-related structures were negatively stained with uranyl acetate for electron microscopy (EM) observation as described by Steven et al. (1988).

Measurement of SPP1 Binding

Measurements of SPP1 reversible and irreversible binding to *B. subtilis* were carried out as previously described (Baptista et al., 2008; São-José et al., 2004).

Fluorescence Microscopy and Image Acquisition

Phage DNA visualization in the bacterial cytoplasm was performed as described in Jakutyte et al. (2011). Briefly, an overnight culture of *B. subtilis* GSY10000 strain producing LacI-CFP was diluted 1:50 in fresh LB, pH 8 medium and grown at 37 °C to A_{600} of 0.8. The culture was supplemented with 5 mM $CaCl_2$, infected at an input multiplicity of 5 with SPP1*delX110lacO*$_{64}$ followed by incubation for 5 min at 37 °C and microscopy at room temperature. The intracellular phage DNA visualization experiment was carried out also in presence of 0.25 mM and 1 mM $CaCl_2$ or in absence of additional $CaCl_2$.

Irreversible phage binding visualization was performed as described in Jakutyte et al. (2011). Briefly, an overnight culture of *B. subtilis* YB886 strain was diluted 1:50 in fresh LB medium and grown at 37 °C to A_{600} of 0.8. Qdot655 streptavidin conjugate (Invitrogen) was added to the chemically modified using EZ-Link Sulfo-NHC-LC-Biotin (Pierce) viable and disrupted phages, immediately prior to use, to obtain the Qdot streptavidin conjugate concentration of 10 nM. The *B. subtilis* culture was supplemented with 10 mM $CaCl_2$ and infected with an input multiplicity of 6 infective phages per bacterium or with the same volume of disrupted phages, incubated for 2 min at 37 °C, fixed with glutaraldehyde to a final concentration of 0.5%, and further incubated at room temperature for 2 min. Fixed bacterium-phage mixtures were diluted 100-fold with TBT buffer, sedimented for 5 min at 5,000×*g*, resuspended in 10 μl of TBT buffer and immediately imaged by contrast and fluorescence microscopy.

Image acquisition and analyses were carried out as described previously (Jakutyte et al., 2011).

Supplementary materials related to this article can be found online at doi:10.1016/j.virol.2011.11.010.

Acknowledgments

We are indebted to Prof. Mário A Santos for communication of unpublished results. *B. subtilis* strain 12A was kindly provided by Prof Shelley Grimes (University Of Minnesota, Minneapolis). L. Jakutyte was supported by the University of Vilnius, Université Paris-Sud, the French embassy in Lithuania, the program Egide Gilibert between France and Lithuania, the European Union Erasmus Program, and by the Région Ile-de-France (SETCI). C. Baptista was supported by the post-doc fellowship SFRH/BPD/34892/2007 from Fundação para a Ciência e a Tecnologia (FCT, MCTES, Portugal). Research was funded by the CNRS, INRA, IFR115, the Research Council of Lithuania (MIP-128/2010) and FCT, MCTES, Portugal, through grant PTDC/BIA-MIC/66412/2006 (to C. São-José).

References

Abdallah, A.M., Gey van Pittius, N.C., Champion, P.A., Cox, J., Luirink, J., Vandenbroucke-Grauls, C.M., Appelmelk, B.J., Bitter, W., 2007. Type VII secretion-mycobacteria show the way. Nat. Rev. Microbiol. 5, 883–891.

Adams, M.H., 1959. Bacteriophages. Wiley Interscience, New York.

Anderson, D.L., Hickman, D.D., Reilly, B.E., 1966. Structure of *Bacillus subtilis* bacteriophage ϕ29 and the length of ϕ29 deoxyribonucleic acid. J. Bacteriol. 91, 2081–2089.

Baptista, C., Santos, M.A., São-José, C., 2008. Phage SPP1 reversible adsorption to *Bacillus subtilis* cell wall teichoic acids accelerates virus recognition of membrane receptor YueB. J. Bacteriol. 190, 4989–4996.

Bonhivers, M., Letellier, L., 1995. Calcium controls phage T5 infection at the level of the *Escherichia coli* cytoplasmic membrane. FEBS Lett. 374, 169–173.

Boulanger, P., Letellier, L., 1988. Characterization of ion channels involved in the penetration of phage T4 DNA into *Escherichia coli* cells. J. Biol. Chem. 263, 9767–9775.

Boulanger, P., Letellier, L., 1992. Ion channels are likely to be involved in the two steps of phage T5 DNA penetration into *Escherichia coli* cells. J. Biol. Chem. 267, 3168–3172.

Chen, C., Guo, P., 1997. Magnesium-induced conformational change of packaging RNA for procapsid recognition and binding during phage phi29 DNA encapsidation. J. Virol. 71, 495–500.

Cvirkaite-Krupovic, V., Krupovic, M., Daugelavicius, R., Bamford, D.H., 2010. Calcium ion-dependent entry of the membrane-containing bacteriophage PM2 into its *Pseudoalteromonas* host. Virology 405, 120–128.

Daugelavicius, R., Bamford, J.K., Bamford, D.H., 1997. Changes in host cell energetics in response to bacteriophage PRD1 DNA entry. J. Bacteriol. 179, 5203–5210.

Duckworth, D.H., Winkler, H.H., 1972. Metabolism of T4 bacteriophage ghost-infected cells. II. Do ghosts cause a generalized permeability change? J. Virol. 9, 917–922.

Gaidelyte, A., Cvirkaite-Krupovic, V., Daugelavicius, R., Bamford, J.K., Bamford, D.H., 2006. The entry mechanism of membrane-containing phage Bam35 infecting *Bacillus thuringiensis*. J. Bacteriol. 188, 5925–5934.

Garcia, L.R., Molineux, I.J., 1996. Transcription-independent DNA translocation of bacteriophage T7 DNA into *Escherichia coli*. J. Bacteriol. 178, 6921–6929.

Goulet, A., Lai-Kee-Him, J., Veesler, D., Auzat, I., Robin, G., Shepherd, D.A., Ashcroft, A.E., Richard, E., Lichière, J., Tavares, P., Cambillau, C., Bron, P., 2011. The opening of the SPP1 bacteriophage tail, a prevalent mechanism in Gram-positive-infecting siphophages. J. Biol. Chem. 286, 25397–25405.

Grahn, A.M., Daugelavicius, R., Bamford, D.H., 2002. Sequential model of phage PRD1 DNA delivery: active involvement of the viral membrane. Mol. Microbiol. 46, 1199–1209.

Grinius, L., Daugelavicius, R., 1988. Depolarization of *Escherichia coli* cytoplasmic membrane by bacteriophages T4 and lambda: evidence for induction of ion-permeable channels. Bioelectrochem. Bioenerg. 19, 235–245.

Hershey, A.D., Chase, M., 1952. Independent functions of viral protein and nucleic acid in growth of bacteriophage. J. Gen. Physiol. 36, 39–56.

Hoch, J.A., Spizizen, J., 1969. Genetic control of some early events in sporulation of *Bacillus subtilis* 168. In: Campbell, L.L. (Ed.), Spores IV. American Society for Microbiology, Bethesda, pp. 112–120.

Jakutyte, L., Baptista, C., São-José, C., Daugelavicius, R., Carballido-López, R., Tavares, P., 2011. Bacteriophage infection in rod-shaped gram-positive bacteria: evidence for a preferential polar route for phage SPP1 entry in *Bacillus subtilis*. J. Bacteriol. 193, 4893–4903.

Labedan, B., Letellier, L., 1981. Membrane potential changes during the first steps of coliphage infection. Proc. Natl. Acad. Sci. U. S. A. 78, 215–219.

Landry, E.F., Zsigray, R.M., 1980. Effects of calcium on the lytic cycle of *Bacillus subtilis* phage 41c. J. Gen. Virol. 51, 125–135.

Lanni, Y.T., 1968. First-step-transfer deoxyribonucleic acid of bacteriophage T5. Bacteriol. Rev. 32, 227–242.

Letellier, L., Labedan, B., 1984. Involvement of envelope-bound calcium in the transient depolarization of the *Escherichia coli* cytoplasmic membrane induced by bacteriophage T4 and T5 adsorption. J. Bacteriol. 157, 789–794.

Letellier, L., Plançon, L., Bonhivers, M., Boulanger, P., 1999. Phage DNA transport across membranes. Res. Microbiol. 150, 499–505.

Moak, M., Molineux, I.J., 2004. Peptidoglycan hydrolytic activities associated with bacteriophage virions. Mol. Microbiol. 51, 1169–1183.

Neuhaus, F.C., Baddiley, J., 2003. A continuum of anionic charge: structures and functions of D-alanyl-teichoic acids in gram-positive bacteria. Microbiol. Mol. Biol. Rev. 67, 686–723.

Nicholls, D., Ferguson, S., 2002. third ed. Bioenergetics, 3. Academic Press, London, United Kingdom.

Okubo, S., Strauss, B., Stodolsky, M., 1964. The possible role of recombination in the infection of competent *Bacillus subtilis* by bacteriophage deoxyribonucleic acid. Virology 24, 552–562.

Petit-Glatron, M.F., Grajcar, L., Munz, A., Chambert, R., 1993. The contribution of the cell wall to a transmembrane calcium gradient could play a key role in *Bacillus subtilis* protein secretion. Mol. Microbiol. 9, 1097–1106.

Plisson, C., White, H.E., Auzat, I., Zafarani, A., São-José, C., Lhuillier, S., Tavares, P., Orlova, E.V., 2007. Structure of bacteriophage SPP1 tail reveals trigger for DNA ejection. EMBO J. 26, 3720–3728.

Poranen, M.M., Daugelavicius, R., Bamford, D.H., 2002. Common principles in viral entry. Annu. Rev. Microbiol. 56, 521–538.

Raspaud, E., Forth, T., São-José, C., Tavares, P., de Frutos, M., 2007. A kinetic analysis of DNA ejection from tailed phages revealing the prerequisite activation energy. Biophys. J. 93, 3999–4005.

Riva, S., Polsinelli, M., Falaschi, A., 1968. A new phage of *Bacillus subtilis* with infectious DNA having separable strands. J. Mol. Biol. 35, 347–356.

Rottenberg, H., 1989. Proton electrochemical potential gradient in vesicles, organelles, and prokaryotic cells. Methods Enzymol. 172, 63–84.

Santos, M.A., de Lencastre, H., Archer, L.J., 1984. Homology between phages SPP1, 41c, 22a, ρ15 and SF6 of *Bacillus subtilis*. J. Gen. Virol. 65, 2067–2072.

São-José, C., Baptista, C., Santos, M.A., 2004. *Bacillus subtilis* operon encoding a membrane receptor for bacteriophage SPP1. J. Bacteriol. 186, 8337–8346.

São-José, C., Lhuillier, S., Lurz, R., Melki, R., Lepault, J., Santos, M.A., Tavares, P., 2006. The ectodomain of the viral receptor YueB forms a fiber that triggers ejection of bacteriophage SPP1 DNA. J. Biol. Chem. 281, 11464–11470.

São-José, C., de Frutos, M., Raspaud, E., Santos, M.A., Tavares, P., 2007. Pressure built by DNA packing inside virions: enough to drive DNA ejection in vitro, largely insufficient for delivery into the bacterial cytoplasm. J. Mol. Biol. 374, 346–355.

Sciara, G., Bebeacua, C., Bron, P., Tremblay, D., Ortiz-Lombardia, M., Lichière, J., van Heel, M., Campanacci, V., Moineau, S., Cambillau, C., 2010. Structure of lactococcal phage p2 baseplate and its mechanism of activation. Proc. Natl. Acad. Sci. U. S. A. 107, 6852–6857.

Silhavy, T.J., Kahne, D., Walker, S., 2010. The bacterial cell envelope. Cold Spring Harb. Perspect. Biol. 2, a000414.

Steensma, H.Y., Blok, J., 1979. Effect of calcium ions on the infection of *Bacillus subtilis* by bacteriophage SF6. J. Gen. Virol. 42, 305–314.

Steven, A.C., Trus, B.L., Maizel, J.V., Unser, M., Parry, D.A., Wall, J.S., Hainfeld, J.F., Studier, F.W., 1988. Molecular substructure of a viral receptor-recognition protein. The gp17 tail-fiber of bacteriophage T7. J. Mol. Biol. 200, 351–365.

Tavares, P., Santos, M.A., Lurz, R., Morelli, G., de Lencastre, H., Trautner, T.A., 1992. Identification of a gene in *Bacillus subtilis* bacteriophage SPP1 determining the amount of packaged DNA. J. Mol. Biol. 225, 81–92.

Tavares, P., Lurz, R., Stiege, A., Rückert, B., Trautner, T.A., 1996. Sequential headful packaging and fate of the cleaved DNA ends in bacteriophage SPP1. J. Mol. Biol. 264, 954–967.

Veesler, D., Robin, G., Lichière, J., Auzat, I., Tavares, P., Bron, P., Campanacci, V., Cambillau, C., 2010. Crystal structure of bacteriophage SPP1 distal tail protein (gp 19.1): a baseplate hub paradigm in gram-positive infecting phages. J. Biol. Chem. 285, 36666–36673.

Vinga, I., São-José, C., Tavares, P., Santos, M.A., 2006a. Bacteriophage entry in the host cell. In: Wegrzyn, G. (Ed.), Modern Bacteriophage Biology and Biotechnology. Research Signpost, Kerala, India, pp. 165–203.

Vinga, I., Dröge, A., Stiege, A.C., Lurz, R., Santos, M.A., Daugelavicius, R., Tavares, P., 2006b. The minor capsid protein gp7 of bacteriophage SPP1 is required for efficient infection of *Bacillus subtilis*. Mol. Microbiol. 61, 1609–1621.

Winkler, H.H., Duckworth, D.H., 1971. Metabolism of T4 bacteriophage ghost-infected cells: effect of bacteriophage and ghosts on the uptake of carbohydrates in *Escherichia coli* B. J. Bacteriol. 107, 259–267.

Yasbin, R.E., Maino, V.C., Young, F.E., 1976. Bacteriophage resistance in *Bacillus subtilis* 168, W23, and interstrain transformants. J. Bacteriol. 125, 1120–1126.

Yasbin, R.E., Fields, P.I., Andersen, B.J., 1980. Properties of *Bacillus subtilis* 168 derivatives freed of their natural prophages. Gene 12, 155–159.

Young, F.E., 1967. Requirement of glucosylated teichoic acid for adsorption of phage in *Bacillus subtilis* 168. Proc. Natl. Acad. Sci. U. S. A. 58, 2377–2384.

Zavriev, S.K., Shemyakin, M.F., 1982. RNA polymerase-dependent mechanism for the stepwise T7 phage DNA transport from the virion into *E. coli*. Nucleic Acids Res. 10, 1635–1652.